DESIGN EDITING FOR OFFLINE MODEL-BASED OPTIMIZATION

Ye Yuan[1, 2*†] **Youyuan Zhang**[1*] **Can (Sam) Chen**[1, 2] **Haolun Wu**[1, 2]

Zixuan (Melody) Li[1, 2] **Jianmo Li**[1] **James J. Clark**[1] **Xue Liu**[1, 2]

[1] McGill University, [2] Mila - Quebec AI Institute

ABSTRACT

Offline model-based optimization (MBO) aims to maximize a black-box objective function using only an offline dataset of designs and scores. These tasks span various domains, such as robotics, material design, and protein and molecular engineering. A common approach involves training a surrogate model using existing designs and their corresponding scores, and then generating new designs through gradient-based updates with respect to the surrogate model. This method suffers from the out-of-distribution issue, where the surrogate model may erroneously predict high scores for unseen designs. To address this challenge, we introduce a novel method, ***D**esign **E**diting for Offline **M**odel-based **O**ptimization* (**DEMO**), which leverages a diffusion prior to calibrate overly optimized designs. DEMO first generates pseudo design candidates by performing gradient ascent with respect to a surrogate model. While these pseudo design candidates contain information beyond the offline dataset, they might be invalid or have erroneously high predicted scores. Therefore, to address this challenge while utilizing the information provided by pseudo design candidates, we propose an editing process to refine these pseudo design candidates. We introduce noise to the pseudo design candidates and subsequently denoise them with a diffusion prior trained on the offline dataset, ensuring they align with the distribution of valid designs. Empirical evaluations on seven offline MBO tasks show that DEMO outperforms various baseline methods, achieving the highest mean rank of 2.1 and a median rank of 1. The source code is provided at here.

1 INTRODUCTION

Designing objects with specific desired traits is a primary goal in many fields, spanning areas such as robotics, material design, and protein and molecular engineering Trabucco et al. (2022); Liao et al. (2019); Sarkisyan et al. (2016); Angermueller et al. (2019); Hamidieh (2018). Conventionally, this goal is pursued by iteratively testing a black-box objective function that maps a design to its property score. However, this process can be costly, time-consuming, or even hazardous Sarkisyan et al. (2016); Angermueller et al. (2019); Hamidieh (2018); Barrera et al. (2016); Sample et al. (2019). Thus, it is more feasible to utilize an existing offline dataset of designs and their scores to find optimal solutions without further real-world testing Trabucco et al. (2022). This approach is known as offline model-based optimization (MBO), where the objective is to identify a design that optimizes the black-box function using only the offline dataset.

Gradient ascent is commonly used to address the offline MBO challenge. For instance, as shown in Figure 1 (a), an offline dataset might consist of five pairs of superconductor materials and their corresponding critical temperature, denoted as $p_{1,2,3,4,5}$. A deep neural network (DNN) model, referred as the *surrogate model* and represented by $f_{\boldsymbol{\theta}}(\cdot)$, is trained to approximate the unknown

*Equal contribution with random order.
†Correspondence: ye.yuan3@mail.mcgill.ca

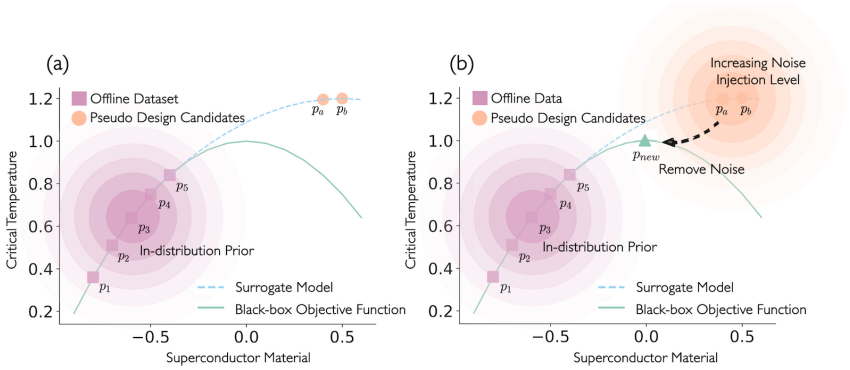

Figure 1: Illustration of DEMO: A diffusion model, acting as the prior distribution, is trained on the offline dataset. Pseudo design candidates are acquired by performing gradient ascent with respect to a learned surrogate model. New designs are generated by modifying pseudo design candidates toward the valid distribution captured by the diffusion prior.

objective function based on this dataset. Gradient ascent is then applied to existing designs with respect to the surrogate model $f_{\boldsymbol{\theta}}(\cdot)$ for generating a new design that achieves a higher score. This approach, however, encounters an out-of-distribution (OOD) problem, where the surrogate struggles to accurately predict data outside the training distribution. This mismatch between the surrogate and the true objective function, as depicted in Figure 1 (a), can result in overly optimistic scores for the new designs generated by gradient ascent Yu et al. (2021).

To tackle this OOD issue, recent research has proposed the use of regularization techniques, either applied directly to the surrogate model Yu et al. (2021); Trabucco et al. (2021); Fu & Levine (2021); Qi et al. (2022a); Yuan et al. (2023); Chen et al. (2023a) or to the design under consideration Chen et al. (2023b;c). These strategies improve the surrogate's robustness and generalization. However, calibrating design candidates generated by gradient ascent remains unexplored. Instead of regularizing the surrogate models, we could tailor these design candidates toward a prior distribution and avoid over optimization.

In this work, we introduce an innovative and effective approach, ***D**esign **E**diting for Offline **M**odel-based **O**ptimization* (**DEMO**) to fill this gap. Initially, a surrogate model, represented as $f_{\boldsymbol{\theta}}(\cdot)$, is trained on the offline dataset $\mathcal{D}$, and gradient ascent is applied to existing designs with respect to the surrogate model. This process generates several designs which may have wrongly high predicted scores but low ground-truth scores due to the inaccuracies of the surrogate model, and we denote them as *pseudo design candidates*. As illustrated in Figure 1 (a), the surrogate model fits the offline data p_1 to p_5, generating pseudo design candidates p_a and p_b through gradient ascent. While these pseudo design candidates might be overly optimized, they contain information beyond the offline dataset. We then propose the second phase to calibrate these pseudo design candidates and align them with the in-distribution area. Specifically, a conditional diffusion model, denoted $s_{\boldsymbol{\phi}}(\cdot)$, is trained on all existing designs along their corresponding scores within the offline dataset to characterize a manifold of valid designs, as all existing designs are valid. After that, we edit the pseudo design candidates by introducing random noise to them and employing the diffusion prior to remove the noise. Comparing to directly leveraging a generative model to craft new design candidates from pure noise, our method benefits from the pseudo design candidates, which incorporate more information than the generative model merely trained on the offline dataset. As illustrated in Figure 1 (b), after injecting noise, the distribution of pseudo design candidates (represented by the orange contour) has more overlap with the valid design distribution (represented by the purple contour). By progressively removing the noise, we gradually project these pseudo design candidates to the manifold of valid designs, as demonstrated in Figure 1 (b). In essence, DEMO produces new designs which are first wildly optimized and then calibrated under the constraints captured by the diffusion prior. We empirically validate DEMO across different offline MBO tasks.

In summary, this paper makes three principal contributions: (i) We introduce a novel method, ***D**esign **E**diting for Offline **M**odel-based **O**ptimization* (**DEMO**). DEMO first performs gradient ascent with respect to a learned surrogate model and share the information to the second phase of DEMO through pseudo design candidates. (ii) The second phase trains a conditional diffusion model on the offline dataset as the in-distribution prior and calibrate the pseudo design candidates with this diffusion prior to generate final designs. (iii) Extensive experiments demonstrate DEMO effectively and reliably generates new designs, yielding state-of-the-art results across 7 offline MBO tasks, with the mean rank of 2.1 and the median rank of 1 among 19 methods.

2 PRELIMINARY

2.1 OFFLINE MODEL-BASED OPTIMIZATION

Offline model-based optimization (MBO) addresses a range of optimization challenges with the aim of maximizing a black-box objective function based on an offline dataset. Mathematically, we define the valid design space as $\mathcal{X} = \mathbb{R}^d$, with d representing the dimension of the design. Offline MBO is formulated as:

$$\boldsymbol{x}^* = \arg\max_{\boldsymbol{x}\in\mathcal{X}} f(\boldsymbol{x}), \tag{1}$$

where $f(\cdot)$ is the black-box objective function, and $\boldsymbol{x} \in \mathcal{X}$ is a potential design. For the optimization process, we utilize an offline dataset $\mathcal{D} = \{(\boldsymbol{x}_i, y_i)\}_{i=1}^N$, with $\boldsymbol{x}_i$ representing an existing design, such as a superconductor material, and y_i representing the associated property score, such as the critical temperature. Usually, this optimization process outputs K candidates for optimal designs, where K is a small budget to test the black-box objective function. The offline MBO problem also finds applications in other areas, like robot design, as well as protein and molecule engineering.

A prevalent approach to solving offline MBO involves approximating the unknown objective function $f(\cdot)$ with a surrogate function, typically a deep neural network (DNN) $f_{\boldsymbol{\theta}}(\cdot)$, trained on $\mathcal{D}$:

$$\boldsymbol{\theta}^* = \arg\min_{\boldsymbol{\theta}} \frac{1}{N}\sum_{i=1}^{N} \left(f_{\boldsymbol{\theta}}(\boldsymbol{x}_i) - y_i\right)^2. \tag{2}$$

Once the surrogate is trained, design optimization is performed using gradient ascent:

$$\boldsymbol{x}_t = \boldsymbol{x}_{t-1} + \eta \nabla_{\boldsymbol{x}} f_{\boldsymbol{\theta}}(\boldsymbol{x})\Big|_{\boldsymbol{x}=\boldsymbol{x}_{t-1}}, \quad \text{for } t \in [1, T]. \tag{3}$$

Here, T represents the number of steps, and η denotes the learning rate. The optimal design $\boldsymbol{x}^*$ is identified as $\boldsymbol{x}_T$. This method faces an *out-of-distribution (OOD) issue*, where the surrogate may fail to accurately predict the scores of unseen designs, resulting in suboptimal solutions.

2.2 DIFFUSION MODELS

Diffusion models stand out in the family of generative models due to their unique approach involving forward diffusion and backward denoising processes. The essence of diffusion models is to gradually add noise to a sample, followed by training a neural network to reverse this noise addition, thus recovering the original data distribution. In this work, we follow the formulation of diffusion models with continuous time Song et al. (2021); Huang et al. (2021). Here, $\boldsymbol{x}(t)$ is a random variable denoting the state of a data point at time $t \in [0, T]$. The diffusion process is defined by a stochastic differential equation (SDE):

$$\mathrm{d}\boldsymbol{x} = \boldsymbol{f}(\boldsymbol{x}, t)\mathrm{d}t + g(t)\mathrm{d}\boldsymbol{w}, \tag{4}$$

where $\boldsymbol{f}(\cdot, t)$ is the drift coefficient, $g(\cdot)$ is the diffusion coefficient, and $\boldsymbol{w}$ is a standard Wiener process. The backward denoising process is given by the reverse time SDE:

$$\mathrm{d}\boldsymbol{x} = \left[\boldsymbol{f}(\boldsymbol{x}, t) - g(t)^2 \nabla_{\boldsymbol{x}} \log p_t(\boldsymbol{x})\right] \mathrm{d}t + g(t)\, \mathrm{d}\bar{\boldsymbol{w}}, \tag{5}$$

where $\mathrm{d}t$ represents a negative infinitesimal step in time, and $\bar{w}$ is a reverse time Wiener process. The gradient of the log probability, $\nabla_{\boldsymbol{x}} \log p_t(\boldsymbol{x})$, is approximated by a neural network $s_{\boldsymbol{\phi}}(\boldsymbol{x}(t), t)$ with score-matching objectives Vincent (2011); Song & Ermon (2020).

Beyond basic diffusion models, our focus is to train a conditional diffusion model that learns the conditional probability distribution of designs based on their associated property scores. To incorporate conditions to diffusion models, Ho et al. Ho & Salimans (2022) achieve it by dividing the score function into a combination of conditional and unconditional components, known as classifier-free diffusion models. Specifically, a single neural network, $s_{\boldsymbol{\phi}}(\boldsymbol{x}_t, t, y)$, is trained to handle both components by utilizing y as the condition or leaving it empty for unconditional functions. Formally, we can write this combination as follows:

$$s_{\boldsymbol{\phi}}(\boldsymbol{x}_t, t, y) = (1 + \omega) s_{\boldsymbol{\phi}}(\boldsymbol{x}_t, t, y) - \omega s_{\boldsymbol{\phi}}(\boldsymbol{x}_t, t), \tag{6}$$

where ω is a parameter that adjusts the influence of the conditions. A higher value of ω ensures that the generation process adheres more closely to the specified conditions, while a lower ω value allows greater flexibility in the outputs.

3 METHODOLOGY

In this section, we elaborate on the details of our proposed ***D**esign **E**diting for Offline **M**odel-based **O**ptimization* (**DEMO**). Typically, the out-of-distribution (OOD) issue in offline MBO arises due to incomplete observation of the entire distribution of designs and scores. During gradient ascent optimization, the pseudo design candidates are optimized with respect to the surrogate model without constraints, which leads them into the OOD region and causes overestimation of the scores. To address this, we introduce a design editing process to calibrate the pseudo design candidates toward the in-distribution area, which mitigates the OOD problem through the use of a learned diffusion prior. Algorithm 1 illustrates the complete process of DEMO.

3.1 ACQUIREMENT OF PSEUDO DESIGN CANDIDATES

Initially, a deep neural network (DNN), denoted as $f_{\boldsymbol{\theta}}(\cdot)$ with parameters $\boldsymbol{\theta}$, is trained on the offline dataset $\mathcal{D} = \{(\boldsymbol{x}_i, y_i)\}_{i=1}^N$, where $\boldsymbol{x}_i$ and y_i denote a design and its associated score, respectively. The parameters $\boldsymbol{\theta}$ are optimized as shown in Eq. (2). The solution $f_{\boldsymbol{\theta}^*}(\cdot)$ obtained from Eq. (2) serves as a surrogate for the unknown black-box objective function $f(\cdot)$ in Eq. (1). New data are then generated by performing gradient ascent on the existing designs with respect to the learned surrogate model $f_{\boldsymbol{\theta}^*}(\cdot)$. The initial point $\boldsymbol{x}_0$ is an existing design selected from $\mathcal{D}$. We update it as shown in Eq. (3). The design $\boldsymbol{x}_T$ acquired at step T is an overly optimized design, as no constraints are applied during the optimization process. By iteratively using the top K designs in the offline dataset $\mathcal{D}$ as the initial points, a batch of pseudo design candidates, denoted as $\mathcal{D}'$, is acquired. This process is outlined from line 2 to line 8 in Algorithm 1.

3.2 TRAINING OF DIFFUSION PRIOR

We employ a classifier-free conditional diffusion model Ho & Salimans (2022) to learn the conditional probability distribution of existing designs and their scores in offline dataset $\mathcal{D}$. Following the approach in DDOM Krishnamoorthy et al. (2023a), we use the Variance Preserving (VP) stochastic differential equation (SDE) for the forward diffusion process, as specified in Song et al. (2021):

$$\mathrm{d}\boldsymbol{x} = -\frac{\beta(t)}{2}\boldsymbol{x}\mathrm{d}t + \sqrt{\beta(t)}\mathrm{d}\boldsymbol{w}, \tag{7}$$

where $\beta(t)$ is a continuous time function for $t \in [0, 1]$. The forward process in DDPM Ho et al. (2020) is proved to be a discretization of Eq. (7) Song et al. (2021). To integrate conditions in the backward denoising process, we need to train a DNN $s_{\boldsymbol{\phi}}(\boldsymbol{x}_t, t, y)$ with parameters $\boldsymbol{\phi}$, conditioned on the time t and the score y associated with the unperturbed design $\boldsymbol{x}_0$ corresponding to $\boldsymbol{x}_t$. The parameters $\boldsymbol{\phi}$ are optimized as:

$$\boldsymbol{\phi}^* = \arg\min_{\boldsymbol{\phi}} \mathbb{E}_t \left[\lambda(t)\mathbb{E}_{\boldsymbol{x}_0,y}\left[\mathbb{E}_{\boldsymbol{x}_t|\boldsymbol{x}_0}\left[\|\boldsymbol{s}_{\boldsymbol{\phi}}(\boldsymbol{x}_t, t, y) - \nabla_{\boldsymbol{x}} \log p_t(\boldsymbol{x}_t|\boldsymbol{x}_0)\|^2\right]\right]\right], \tag{8}$$

where $\lambda(t)$ is a positive weighting function depending on time. Since we train on the offline dataset $\mathcal{D}$, the model optimized according to Eq. (8) captures the manifold of valid designs. This part is described in Line 10 of Algorithm 1.

However, since the offline dataset may contain very low-score existing designs, naively applying the trained model to the subsequent design editing process might be harmful for calibrating the pseudo design candidates. Therefore, we propose to use the distribution conditioned on the maximum property score among the offline dataset as the prior for later usage, which is a simple yet effective method for mitigating the negative impacts of very low-score designs.

3.3 DESIGN EDITING PROCESS

Due to potential inaccuracies of the surrogate model $f_{\boldsymbol{\theta}^*}(\cdot)$ in representing the black-box objective function, the set of pseudo design candidates $\mathcal{D}'$ might include samples that have high predicted scores but low ground-truth scores. Inspired by the success of editing techniques in image synthesis tasks Meng et al. (2022); Su et al. (2023), we explore the potential of calibrating these pseudo design candidates to obtain new designs with valid high scores. We perturb a pseudo design candidate

$\boldsymbol{x}^{(p)} \in \mathcal{D}'$ by introducing noise at a specific time m out of $\{1, \cdots, M\}$ and auxiliary noise levels $\beta_1, \cdots, \beta_M$:

$$\boldsymbol{x}^{(p)}_{\text{perturb}} = \sqrt{\bar{\alpha}_m}\boldsymbol{x}^{(p)} + \sqrt{1-\bar{\alpha}_m}\epsilon, \tag{9}$$

where $\alpha_m = 1 - \beta_m$, $\bar{\alpha}_m = \prod_{s=1}^{m} \alpha_s$, and $\epsilon \sim \mathcal{N}(\mathbf{0}, \mathbf{I})$. This results in a closed-form expression that samples $\boldsymbol{x}^{(p)}_{\text{perturb}} \sim \mathcal{N}(\sqrt{\bar{\alpha}_m}\boldsymbol{x}^{(p)}, (1-\bar{\alpha}_m)\mathbf{I})$. The perturbed design is then used as the starting point. A final optimized design is synthesized by using any numerical solver for the backward denoising process with the model $s_{\boldsymbol{\phi}^*}(\cdot)$, conditioned on the maximum property score among the offline dataset, to remove the noise. In our implementation, we follow existing studies Krishnamoorthy et al. (2023a) and use Heun's method as the solver. To yield K final optimized designs, we utilize all pseudo design candidates from $\mathcal{D}'$, obtain various perturbed designs, and denoise them, pushing them toward the prior distribution. Lines 12 to 17 of Algorithm 1 present the process of this procedure.

Algorithm 1 Design Editing for Offline Model-based Optimization

Input: Offline dataset $\mathcal{D} = \{(\boldsymbol{x}_i, y_i)\}_{i=1}^{N}$, and a time m.
Output: K candidate optimal designs.

1: /* Acquirement of Pseudo Design Candidates */
2: Initialize a surrogate model $f_{\boldsymbol{\theta}}(\cdot)$ and optimize $\boldsymbol{\theta}$ with Eq. (2) to obtain $f_{\boldsymbol{\theta}^*}(\cdot)$.
3: $\mathcal{D}' = \{\}$
4: **for** $i = 1, 2, \cdots, K$ **do**
5: $\quad \boldsymbol{x}_0 \longleftarrow \boldsymbol{x}_i$ with the i-th best score within $\mathcal{D}$.
6: $\quad$ **for** $t = 1, 2, \cdots, T$ **do**
7: $\quad\quad$ Update $\boldsymbol{x}_t$ with Eq. (3).
8: $\quad$ Append $\boldsymbol{x}_T$ to $\mathcal{D}'$.
9: /* Training of Diffusion Prior */
10: Initialize $s_{\boldsymbol{\phi}}(\cdot)$ and optimize $\boldsymbol{\phi}$ with Eq. (8) on $\mathcal{D}$ to obtain $s_{\boldsymbol{\phi}^*}(\cdot)$.
11: /* Design Editing Process */
12: Candidates = $\{\}$
13: **for** $i = 1, 2, \cdots, K$ **do**
14: $\quad \boldsymbol{x}^{(p)} \longleftarrow \boldsymbol{x}_i \in \mathcal{D}'$
15: $\quad$ Perturb $\boldsymbol{x}^{(p)}$ with Eq. (9) and the given time m.
16: $\quad$ Denoise $\boldsymbol{x}^{(p)}_{perturb}$ and generate $\boldsymbol{x}_{new}$ using the Heun's method with $s_{\boldsymbol{\phi}^*}(\cdot)$ conditioned on $\max(\{y_i\}_{i=1}^{N})$.
17: $\quad$ Append $\boldsymbol{x}_{new}$ to Candidates.
18: **return** Candidates

4 Experiments

This section first describes the experiment setup, followed by the implementation details and results. We aim to answer the following questions in this section: *(Q1)* Is our proposed DEMO more effective than baseline methods in addressing the offline MBO problem? *(Q2)* One can alternatively generate new designs from the diffusion prior or directly use the pseudo design candidates. Is DEMO better than these partial alternatives by introducing the editing process?

4.1 Dataset and Tasks

We carry out experiments on 7 tasks selected from Design-Bench Trabucco et al. (2022) and BayesO Benchmarks Kim (2023), including 4 continuous tasks and 3 discrete tasks. The continuous tasks are as follows: *(i)* Superconductor (SuperC) Hamidieh (2018), where the goal is to create a superconductor with 86 continuous components to maximize critical temperature, using $17,010$ designs; *(ii)* Ant Morphology (Ant) Trabucco et al. (2022); Brockman et al. (2016), where the objective is to design a four-legged ant with 60 continuous components to increase crawling speed, based on $10,004$ designs; *(iii)* D'Kitty Morphology (D'Kitty) Trabucco et al. (2022); Ahn et al. (2020), where the focus is on designing a four-legged D'Kitty with 56 continuous components to enhance crawling speed, using $10,004$ designs; *(iv)* Inverse Levy Function (Levy) Kim (2023), where the aim is to maximize

function values of the inverse black-box Levy function with 60 input dimensions, using $15,000$ designs. The discrete tasks include: *(v)* TF Bind 8 (TF8) Barrera et al. (2016), where the goal is to identify an 8-unit DNA sequence that maximizes binding activity score, with $32,898$ designs; *(vi)* TF Bind 10 (TF10) Barrera et al. (2016), where the objective is to find a 10-unit DNA sequence that optimizes binding activity score, using $50,000$ designs; *(vii)* NAS Zoph & Le (2017), where the aim is to discover the optimal neural network architecture to improve test accuracy on the CIFAR-10 dataset Hinton et al. (2012), using $1,771$ designs.

4.2 Evaluation and Metrics

Following the evaluation protocol used in previous studies Trabucco et al. (2022), we assume the budget $K = 128$ and generate 128 new designs for each method. The 100-th (max) percentile normalized ground-truth score is reported in this section, and the 50-th (median) percentile score is provided in Appendix A.2. This normalized score is calculated as $y_n = \frac{y - y_{\min}}{y_{\max} - y_{\min}}$, where $y_{\min}$ and $y_{\max}$ are the minimum and maximum scores in the entire offline dataset, respectively. For better comparison, we include the normalized score of the best design in the offline dataset, denoted as $\mathcal{D}(\textbf{best})$. Additionally, we provide mean and median rankings across all 7 tasks for a comprehensive performance evaluation.

4.3 Comparison Methods

We benchmark DEMO against three groups of baseline approaches: *(i)* traditional methods, *(ii)* those utilizing gradient optimizations from current designs, and *(iii)* those employing generative models for sampling. Traditional methods include: *(1)* **BO-qEI** Wilson et al. (2017): conducts Bayesian Optimization to maximize the surrogate, proposes designs using the quasi-Expected-Improvement acquisition function, and labels the designs using the surrogate model. *(2)* **CMA-ES** Hansen (2006): progressively adjusts the distribution toward the optimal design by altering the covariance matrix. *(3)* **REINFORCE** Williams (1992): optimizes the distribution over the input space using the learned surrogate. The second category includes: *(4)* **Mean**: optimizes the average prediction of the ensemble of surrogate models. *(5)* **Min**: optimizes the lowest prediction from a group of learned objective functions. *(6)* **COMs** Trabucco et al. (2021): applies regularization to assign lower scores to designs derived through gradient ascent. *(7)* **ROMA** Yu et al. (2021): introduces smoothness regularization to the DNN. *(8)* **NEMO** Fu & Levine (2021): limits the discrepancy between the surrogate and the black-box objective function using normalized maximum likelihood before performing gradient ascent. *(9)* **BDI** Chen et al. (2023b) employs forward and backward mappings to transfer knowledge from the offline dataset to the design. *(10)* **IOM** Qi et al. (2022b): ensures representation consistency between the training dataset and the optimized designs. *(11)* **ICT** Yuan et al. (2023): identifies useful information from a pseudo-labeled dataset to improve the surrogate model. *(12)* **Tri-mentoring** Chen et al. (2023a): leverages information of pairwise comparison data to enhance ensemble performance. *(13)* **PGS** Chemingui et al. (2024): learns the best policy for a given surrogate model. Generative model-based methods include: *(14)* **CbAS** Brookes et al. (2019), which adapts a VAE model to steer the design distribution toward areas with higher scores. *(15)* **Auto CbAS** Fannjiang & Listgarten (2020), which uses importance sampling to update a regression model based on CbAS. *(16)* **MIN** Kumar & Levine (2020), which establishes a relationship between scores and designs and seeks optimal designs within this framework. *(17)* **DDOM** Krishnamoorthy et al. (2023a), which learns a generative diffusion model conditioned on the score values. *(18)* **BONET** Krishnamoorthy et al. (2023b), which employs an autoregressive model trained on the offline dataset.

4.4 Implementation Details

We follow the training protocols from Trabucco et al. (2021) for all comparative methods unless stated otherwise. A 3-layer MLP with ReLU activation is used for both $f_{\boldsymbol{\theta}}(\cdot)$ and $s_{\boldsymbol{\phi}}(\cdot)$, with a hidden layer size of 2048. In Algorithm 1, the iteration count, T, is established at 100 for both continuous and discrete tasks. The Adam optimizer Kingma & Ba (2017) is utilized to train the surrogate models over 200 epochs with a batch size of 128, and a learning rate set at $1e-1$. The step size, η, in Eq. (3) is configured at $1e-3$ for continuous tasks and $1e-1$ for discrete tasks. The diffusion model, $s_{\boldsymbol{\phi}}(\cdot)$, undergoes training for 1000 epochs with a batch size of 128. For the *design editing process*, following precedents set by previous studies Krishnamoorthy et al. (2023a),

Table 1: Experimental results on continuous tasks for comparison.

Method	Superconductor	Ant Morphology	D'Kitty Morphology	Levy
$\mathcal{D}$(**best**)	0.399	0.565	0.884	0.613
BO-qEI	0.402 ± 0.034	0.819 ± 0.000	0.896 ± 0.000	0.810 ± 0.016
CMA-ES	0.465 ± 0.024	$\mathbf{1.214 \pm 0.732}$	0.724 ± 0.001	0.887 ± 0.025
REINFORCE	0.481 ± 0.013	0.266 ± 0.032	0.562 ± 0.196	0.564 ± 0.090
Mean	0.505 ± 0.013	0.940 ± 0.014	$\mathbf{0.956 \pm 0.014}$	$\mathbf{0.984 \pm 0.023}$
Min	0.501 ± 0.019	0.918 ± 0.034	0.942 ± 0.009	0.964 ± 0.023
COMs	0.481 ± 0.028	0.842 ± 0.037	0.926 ± 0.019	0.936 ± 0.025
ROMA	0.509 ± 0.015	0.916 ± 0.030	0.929 ± 0.013	0.976 ± 0.019
NEMO	0.502 ± 0.002	0.955 ± 0.006	0.952 ± 0.004	0.969 ± 0.019
BDI	0.513 ± 0.000	0.906 ± 0.000	0.919 ± 0.000	0.938 ± 0.000
IOM	$\mathbf{0.518 \pm 0.020}$	0.922 ± 0.030	0.944 ± 0.012	$\mathbf{0.988 \pm 0.021}$
ICT	0.503 ± 0.017	$\mathbf{0.961 \pm 0.007}$	$\mathbf{0.968 \pm 0.020}$	0.879 ± 0.018
Tri-mentoring	$\mathbf{0.514 \pm 0.018}$	0.948 ± 0.014	$\mathbf{0.966 \pm 0.010}$	0.924 ± 0.035
PGS	$\mathbf{0.563 \pm 0.058}$	0.949 ± 0.017	$\mathbf{0.966 \pm 0.013}$	0.963 ± 0.027
CbAS	$\mathbf{0.503 \pm 0.069}$	0.876 ± 0.031	0.892 ± 0.008	0.938 ± 0.037
Auto CbAS	0.421 ± 0.045	0.882 ± 0.045	0.906 ± 0.006	0.797 ± 0.033
MIN	0.499 ± 0.017	0.445 ± 0.080	0.892 ± 0.011	0.761 ± 0.037
DDOM	0.486 ± 0.013	0.952 ± 0.007	0.941 ± 0.006	0.927 ± 0.031
BONET	0.437 ± 0.022	$\mathbf{0.976 \pm 0.012}$	0.954 ± 0.012	0.918 ± 0.025
DEMO$_{(\text{ours})}$	$\mathbf{0.525 \pm 0.009}$	$\mathbf{0.968 \pm 0.009}$	$\mathbf{0.970 \pm 0.007}$	$\mathbf{1.007 \pm 0.015}$

Table 2: Experimental results on discrete tasks, and ranking on all tasks for comparison.

Method	TF Bind 8	TF Bind 10	NAS	Rank Mean	Rank Median
$\mathcal{D}$(**best**)	0.439	0.467	0.436		
BO-qEI	0.798 ± 0.083	0.652 ± 0.038	$\mathbf{1.079 \pm 0.059}$	13.9/19	16/19
CMA-ES	0.953 ± 0.022	0.670 ± 0.023	0.985 ± 0.079	9.1/19	7/19
REINFORCE	0.948 ± 0.028	0.663 ± 0.034	-1.895 ± 0.000	15.1/19	19/19
Mean	0.895 ± 0.020	0.654 ± 0.028	0.663 ± 0.058	9.3/19	9/19
Min	0.931 ± 0.036	0.634 ± 0.033	0.708 ± 0.027	10.7/19	11/19
COMs	0.474 ± 0.053	0.625 ± 0.010	0.796 ± 0.029	13.1/19	14/19
ROMA	0.921 ± 0.040	0.669 ± 0.035	0.934 ± 0.025	7.9/19	7/19
NEMO	0.942 ± 0.003	$\mathbf{0.708 \pm 0.010}$	0.735 ± 0.012	6.7/19	7/19
BDI	0.870 ± 0.000	0.605 ± 0.000	0.722 ± 0.000	12.1/19	13/19
IOM	0.870 ± 0.074	0.648 ± 0.025	0.411 ± 0.044	10.0/19	10/19
ICT	0.958 ± 0.008	0.691 ± 0.023	0.667 ± 0.091	7.7/19	6/19
Tri-mentoring	$\mathbf{0.970 \pm 0.001}$	$\mathbf{0.722 \pm 0.017}$	0.759 ± 0.102	5.4/19	4/19
PGS	$\mathbf{0.981 \pm 0.015}$	0.658 ± 0.021	0.727 ± 0.033	5.4/19	7/19
CbAS	0.927 ± 0.051	0.651 ± 0.060	0.683 ± 0.079	12.0/19	12/19
Auto CbAS	0.910 ± 0.044	0.630 ± 0.045	0.506 ± 0.074	15.6/19	16/19
MIN	0.905 ± 0.052	0.616 ± 0.021	0.717 ± 0.046	15.4/19	16/19
DDOM	0.961 ± 0.024	0.640 ± 0.029	0.737 ± 0.014	9.4/19	10/19
BONET	$\mathbf{0.975 \pm 0.004}$	0.681 ± 0.035	0.724 ± 0.008	8.0/19	6/19
DEMO$_{(\text{ours})}$	$\mathbf{0.982 \pm 0.016}$	$\mathbf{0.762 \pm 0.058}$	0.753 ± 0.017	**2.1/19**	**1/19**

we set M at 1000. The selected value of m is 600, with further elaboration provided in Appendix A.3. Results from traditional methodologies are referenced from Trabucco et al. (2022), and we conduct 8 independent trials for other methods, reporting the mean and standard error. All experiments are conducted on a single NVIDIA V100 GPU, with execution times per trial ranging from 10 minutes to 20 hours, depending on the specific tasks.

4.5 RESULTS

Performance in Continuous Tasks. Table 1 presents the results of the four continuous tasks. DEMO achieves state-of-the-art performance across all of them. DEMO outperforms gradient-based methods, such as NEMO and ICT, by leveraging the design editing process to calibrate the pseudo design candidates rather than performing unconstrained optimization against regularized surrogate models. It is worth noting that some methods, such as COMs, employ a constrained optimization process by penalizing the value at a lookahead gradient ascent optimization point. The superior performance of DEMO compared to COMs indicates that the design editing process is a more effective method. Moreover, when compared to other generative model-based approaches, such as MIN and DDOM, DEMO generally outperforms them because these methods train models solely on

the offline dataset and may not benefit from the information provided by surrogate models. DEMO achieves better performance by effectively utilizing the surrogate model to acquire a batch of pseudo design candidates. These results strongly support the effectiveness of DEMO for continuous tasks.

Performance in Discrete Tasks. Table 2 displays the results of the three discrete tasks. DEMO achieves top performance in TF Bind 8 and TF Bind 10, with the results on TF10 surpassing those of other methods by a significant margin, suggesting DEMO's capability in solving discrete offline MBO tasks. However, DEMO underperforms on NAS, which may be due to two reasons. First, each neural network architecture is encoded as a sequence of one-hot vectors, which has a length of 64. This encoding process might be insufficient for precisely representing all features of a given architecture, leading to suboptimal performance on NAS. Additionally, after examining the NAS offline dataset, we found that many existing designs share commonalities. This redundancy means that the NAS dataset contains less useful information compared to other tasks, which further explains why DEMO's performance on NAS is not as strong.

Summary. These results on both continuous and discrete tasks provide a clear answer to $Q1$. DEMO attains the highest rankings with a mean of 2.1/19 and a median of 1/19, as detailed in Table 2 and Figure 2, and secures top performance in all tasks. We also conduct a Welch's t-test on the tasks where DEMO achieved state-of-the-art results. We obtain p-values of 0.20 on SuperC, 0.04 on Ant, 0.01 on D'Kitty, 0.03 on Levy, 0.03 on TF8, and 0.005 on TF10. This confirms that DEMO achieves statistically significant improvements in 5 out of 7 tasks when setting the significance level $\alpha = 0.05$. We further examine the reliability of DEMO in Appendix A.4.

4.6 Ablation Study

New designs can be alternatively generated from the prior distribution using the diffusion model or by directly using the pseudo design candidates after the gradient ascent process. We refer to these two methods as Diffusion-only and Grad-only, respectively. To rigorously assess whether the introduction of the editing phase within our DEMO method is beneficial, ablation experiments are conducted by systematically comparing the complete DEMO method with Diffusion-only and Grad-only. The results, summarized in Table 3, provide clear insights into the impact of our design editing process. For the four continuous tasks, DEMO consistently achieves higher performance compared to its ablated versions. For instance, in the SuperC task, DEMO achieves a score of 0.525 ± 0.009, significantly higher than both Grad-only (0.482 ± 0.013) and Diffusion-only (0.346 ± 0.011). Unlike baseline methods of conditional generative models based on a target score higher than all existing designs, such as Auto CbAS and DDOM, the Diffusion-only approach generates new designs conditioned on the maximum score within the offline dataset for the ablation study purpose. Similar improvements are observed in the Ant, D'Kitty, and Levy tasks, underscoring the effectiveness of integrating the design editing process in continuous tasks. In the discrete tasks TF8, TF10, and NAS, DEMO's superior performance over both alternative solutions is evident, highlighting its comprehensive effectiveness in managing discrete challenges. Overall, the ablation studies validate the importance of the design editing process within the DEMO method, answering $Q2$ conclusively. The complete DEMO method collectively contributes to enhancements across a range of tasks and various input dimensions.

Table 3: Ablation studies on two phases of DEMO.

Task	D	DEMO	Grad-only	Diffusion-only
SuperC	86	**0.525 ± 0.009**	0.482 ± 0.013	0.346 ± 0.011
Ant	60	**0.968 ± 0.009**	0.963 ± 0.008	0.377 ± 0.004
D'Kitty	56	**0.970 ± 0.007**	0.933 ± 0.002	0.762 ± 0.023
Levy	60	**1.007 ± 0.015**	0.990 ± 0.020	0.483 ± 0.015
TF8	8	**0.980 ± 0.004**	0.965 ± 0.008	0.420 ± 0.004
TF10	10	**0.762 ± 0.058**	0.638 ± 0.019	0.465 ± 0.006
NAS	64	**0.753 ± 0.017**	0.668 ± 0.084	0.274 ± 0.013

5 Conclusion and Discussion

In this study, we introduce ***D**esign **E**diting for Offline **M**odel-based **O**ptimization* (**DEMO**). In essence, DEMO generates new designs by first extensively optimizing pseudo design candidates and then refining them with the diffusion prior trained on the valid region. Extensive experiments on diverse offline MBO tasks validate that DEMO achieves state-of-the-art performance. We discuss the related works in Appendix A.5. The limitations and potential negative impacts are discussed in Appendix A.6 and Appendix A.7, respectively.

REFERENCES

Michael Ahn, Henry Zhu, Kristian Hartikainen, Hugo Ponte, Abhishek Gupta, Sergey Levine, and Vikash Kumar. Robel: Robotics benchmarks for learning with low-cost robots. In Conf. on Robot Lea. (CoRL), 2020.

Christof Angermueller, David Dohan, David Belanger, Ramya Deshpande, Kevin Murphy, and Lucy Colwell. Model-based reinforcement learning for biological sequence design. In Proc. Int. Conf. Learning Rep. (ICLR), 2019.

Luis A Barrera et al. Survey of variation in human transcription factors reveals prevalent dna binding changes. Science, 2016.

Greg Brockman, Vicki Cheung, Ludwig Pettersson, Jonas Schneider, John Schulman, Jie Tang, and Wojciech Zaremba. Openai gym. arXiv preprint arXiv:1606.01540, 2016.

David Brookes, Hahnbeom Park, and Jennifer Listgarten. Conditioning by adaptive sampling for robust design. In Proc. Int. Conf. Machine Lea. (ICML), 2019.

Duygu Ceylan, Chun-Hao P Huang, and Niloy J Mitra. Pix2video: Video editing using image diffusion. In Proceedings of the IEEE/CVF International Conference on Computer Vision, pp. 23206–23217, 2023.

Yassine Chemingui, Aryan Deshwal, Trong Nghia Hoang, and Janardhan Rao Doppa. Offline model-based optimization via policy-guided gradient search, 2024. URL https://arxiv.org/abs/2405.05349.

Can Chen, Christopher Beckham, Zixuan Liu, Xue Liu, and Christopher Pal. Parallel-mentoring for offline model-based optimization, 2023a.

Can Chen, Yingxue Zhang, Jie Fu, Xue Liu, and Mark Coates. Bidirectional learning for offline infinite-width model-based optimization, 2023b.

Can Chen, Yingxue Zhang, Xue Liu, and Mark Coates. Bidirectional learning for offline model-based biological sequence design, 2023c.

Yuren Cong, Mengmeng Xu, Christian Simon, Shoufa Chen, Jiawei Ren, Yanping Xie, Juan-Manuel Perez-Rua, Bodo Rosenhahn, Tao Xiang, and Sen He. Flatten: optical flow-guided attention for consistent text-to-video editing. arXiv preprint arXiv:2310.05922, 2023.

Clara Fannjiang and Jennifer Listgarten. Autofocused oracles for model-based design. Proc. Adv. Neur. Inf. Proc. Syst (NeurIPS), 2020.

Justin Fu and Sergey Levine. Offline model-based optimization via normalized maximum likelihood estimation. Proc. Int. Conf. Learning Rep. (ICLR), 2021.

Michal Geyer, Omer Bar-Tal, Shai Bagon, and Tali Dekel. Tokenflow: Consistent diffusion features for consistent video editing. arXiv preprint arXiv:2307.10373, 2023.

Kam Hamidieh. A data-driven statistical model for predicting the critical temperature of a superconductor. Computational Materials Science, 2018.

Nikolaus Hansen. The CMA evolution strategy: A comparing review. In Towards a New Evolutionary Computation: Advances in the Estimation of Distribution Algorithms, 2006.

Geoffrey E. Hinton, Nitish Srivastava, Alex Krizhevsky, Ilya Sutskever, and Ruslan R. Salakhutdinov. Improving neural networks by preventing co-adaptation of feature detectors. arXiv preprint arXiv:1207.0580, 2012.

Jonathan Ho and Tim Salimans. Classifier-free diffusion guidance, 2022.

Jonathan Ho, Ajay Jain, and Pieter Abbeel. Denoising diffusion probabilistic models, 2020.

Chin-Wei Huang, Jae Hyun Lim, and Aaron Courville. A variational perspective on diffusion-based generative models and score matching, 2021.

Xuan Ju, Ailing Zeng, Yuxuan Bian, Shaoteng Liu, and Qiang Xu. Direct inversion: Boosting diffusion-based editing with 3 lines of code. arXiv preprint arXiv:2310.01506, 2023.

Jungtaek Kim. BayesO Benchmarks: Benchmark functions for Bayesian optimization, 2023.

Diederik P. Kingma and Jimmy Ba. Adam: A method for stochastic optimization, 2017.

Siddarth Krishnamoorthy, Satvik Mehul Mashkaria, and Aditya Grover. Diffusion models for black-box optimization, 2023a.

Siddarth Krishnamoorthy, Satvik Mehul Mashkaria, and Aditya Grover. Generative pretraining for black-box optimization, 2023b. URL https://arxiv.org/abs/2206.10786.

Aviral Kumar and Sergey Levine. Model inversion networks for model-based optimization. Proc. Adv. Neur. Inf. Proc. Syst (NeurIPS), 2020.

Thomas Liao, Grant Wang, Brian Yang, Rene Lee, Kristofer Pister, Sergey Levine, and Roberto Calandra. Data-efficient learning of morphology and controller for a microrobot. arXiv preprint arXiv:1905.01334, 2019.

Chenlin Meng, Yutong He, Yang Song, Jiaming Song, Jiajun Wu, Jun-Yan Zhu, and Stefano Ermon. Sdedit: Guided image synthesis and editing with stochastic differential equations, 2022.

Daiki Miyake, Akihiro Iohara, Yu Saito, and Toshiyuki Tanaka. Negative-prompt inversion: Fast image inversion for editing with text-guided diffusion models. arXiv preprint arXiv:2305.16807, 2023.

Ron Mokady, Amir Hertz, Kfir Aberman, Yael Pritch, and Daniel Cohen-Or. Null-text inversion for editing real images using guided diffusion models. In Proceedings of the IEEE/CVF Conference on Computer Vision and Pattern Recognition, pp. 6038–6047, 2023.

Chenyang Qi, Xiaodong Cun, Yong Zhang, Chenyang Lei, Xintao Wang, Ying Shan, and Qifeng Chen. Fatezero: Fusing attentions for zero-shot text-based video editing. arXiv preprint arXiv:2303.09535, 2023.

Han Qi, Yi Su, Aviral Kumar, and Sergey Levine. Data-driven offline decision-making via invariant representation learning, 2022a. URL https://arxiv.org/abs/2211.11349.

Han Qi, Yi Su, Aviral Kumar, and Sergey Levine. Data-driven model-based optimization via invariant representation learning. In Proc. Adv. Neur. Inf. Proc. Syst (NeurIPS), 2022b.

Paul J Sample, Ban Wang, David W Reid, Vlad Presnyak, Iain J McFadyen, David R Morris, and Georg Seelig. Human 5 UTR design and variant effect prediction from a massively parallel translation assay. Nature Biotechnology, 2019.

Karen S Sarkisyan et al. Local fitness landscape of the green fluorescent protein. Nature, 2016.

Jiaming Song, Chenlin Meng, and Stefano Ermon. Denoising diffusion implicit models, 2022.

Yang Song and Stefano Ermon. Generative modeling by estimating gradients of the data distribution, 2020.

Yang Song, Jascha Sohl-Dickstein, Diederik P. Kingma, Abhishek Kumar, Stefano Ermon, and Ben Poole. Score-based generative modeling through stochastic differential equations, 2021.

Xuan Su, Jiaming Song, Chenlin Meng, and Stefano Ermon. Dual diffusion implicit bridges for image-to-image translation. In International Conference on Learning Representations, 2023.

Brandon Trabucco, Aviral Kumar, Xinyang Geng, and Sergey Levine. Conservative objective models for effective offline model-based optimization, 2021.

Brandon Trabucco, Xinyang Geng, Aviral Kumar, and Sergey Levine. Design-bench: Benchmarks for data-driven offline model-based optimization. arXiv preprint arXiv:2202.08450, 2022.

Pascal Vincent. A connection between score matching and denoising autoencoders. Neural Computation, 23(7):1661–1674, 2011. doi: 10.1162/NECO_a_00142.

Ronald J Williams. Simple statistical gradient-following algorithms for connectionist reinforcement learning. Machine Learning, 1992.

James T Wilson, Riccardo Moriconi, Frank Hutter, and Marc Peter Deisenroth. The reparameterization trick for acquisition functions. arXiv preprint arXiv:1712.00424, 2017.

Chen Henry Wu and Fernando De la Torre. A latent space of stochastic diffusion models for zero-shot image editing and guidance. In Proceedings of the IEEE/CVF International Conference on Computer Vision, pp. 7378–7387, 2023.

Shuai Yang, Yifan Zhou, Ziwei Liu, and Chen Change Loy. Rerender a video: Zero-shot text-guided video-to-video translation. arXiv preprint arXiv:2306.07954, 2023.

Sihyun Yu, Sungsoo Ahn, Le Song, and Jinwoo Shin. Roma: Robust model adaptation for offline model-based optimization. Proc. Adv. Neur. Inf. Proc. Syst (NeurIPS), 2021.

Ye Yuan, Can Chen, Zixuan Liu, Willie Neiswanger, and Xue Liu. Importance-aware co-teaching for offline model-based optimization, 2023.

Youyuan Zhang, Xuan Ju, and James J Clark. Fastvideoedit: Leveraging consistency models for efficient text-to-video editing. arXiv preprint arXiv:2403.06269, 2024.

Barret Zoph and Quoc V. Le. Neural architecture search with reinforcement learning. arXiv preprint arXiv:1611.01578, 2017.

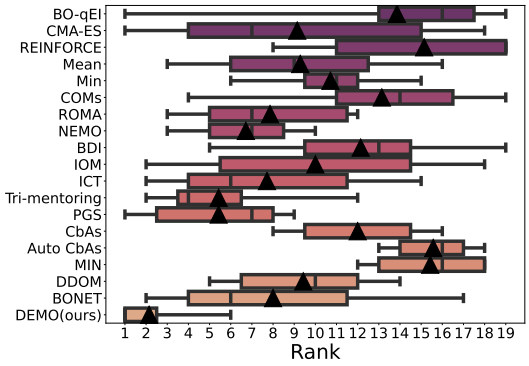

Figure 2: Comparison of ranks across methods.

Table 4: Experimental results on continuous tasks for comparison.

Method	Superconductor	Ant Morphology	D'Kitty Morphology	Levy
$\mathcal{D}$(**best**)	0.399	0.565	0.884	0.613
BO-qEI	0.300 ± 0.015	0.567 ± 0.000	0.883 ± 0.000	0.643 ± 0.009
CMA-ES	0.379 ± 0.003	-0.045 ± 0.004	0.684 ± 0.016	0.410 ± 0.009
REINFORCE	$\mathbf{0.463 \pm 0.016}$	0.138 ± 0.032	0.356 ± 0.131	0.377 ± 0.065
Mean	0.334 ± 0.004	0.569 ± 0.011	0.876 ± 0.005	0.561 ± 0.007
Min	0.364 ± 0.030	0.569 ± 0.021	0.873 ± 0.009	0.537 ± 0.006
COMs	0.316 ± 0.024	0.564 ± 0.002	0.881 ± 0.002	0.511 ± 0.012
ROMA	0.370 ± 0.019	0.477 ± 0.038	0.854 ± 0.007	0.558 ± 0.003
NEMO	0.320 ± 0.008	0.592 ± 0.000	0.883 ± 0.000	0.538 ± 0.006
BDI	0.412 ± 0.000	0.474 ± 0.000	0.855 ± 0.000	0.534 ± 0.003
IOM	0.350 ± 0.023	0.513 ± 0.035	0.876 ± 0.006	0.562 ± 0.007
ICT	0.399 ± 0.012	0.592 ± 0.025	0.874 ± 0.005	0.691 ± 0.009
Tri-mentoring	0.355 ± 0.003	0.606 ± 0.007	0.866 ± 0.001	0.687 ± 0.012
PGS	0.379 ± 0.016	0.532 ± 0.016	$\mathbf{0.941 \pm 0.008}$	0.476 ± 0.014
CbAS	0.111 ± 0.017	0.384 ± 0.016	0.753 ± 0.008	0.479 ± 0.020
Auto CbAS	0.131 ± 0.010	0.364 ± 0.014	0.736 ± 0.025	0.499 ± 0.022
MIN	0.336 ± 0.016	0.618 ± 0.040	0.887 ± 0.004	0.681 ± 0.030
DDOM	0.346 ± 0.009	0.615 ± 0.007	0.861 ± 0.003	0.595 ± 0.012
BONET	0.369 ± 0.015	$\mathbf{0.819 \pm 0.032}$	0.907 ± 0.020	0.604 ± 0.008
DEMO$_{(\text{ours})}$	0.400 ± 0.007	0.604 ± 0.005	$\mathbf{0.891 \pm 0.002}$	$\mathbf{0.762 \pm 0.008}$

A Appendix

A.1 Illustration of Rankings

A.2 Median Normalized Scores

Performance in Continuous Tasks. Table 4 showcases the median normalized scores for various baseline methods across 4 continuous tasks. DEMO, while not always topping the charts, demonstrates robust performance across these tasks, consistently outperforming several baseline methods. For example, in the Levy function task, DEMO's score of 0.762 ± 0.008 is the highest one among all approaches. This highlights DEMO's capability to mitigate the OOD issue of surrogates based methods effectively. Notably, DEMO outperforms traditional generative models like CbAS and Auto CbAS by significant margins across all tasks. It also maintains a competitive edge against more recent generative methods like MIN and DDOM.

Performance in Discrete Tasks. Moving to discrete tasks, as detailed in Table 5, DEMO exhibits performance on par with other baseline methods. This performance can be attributed to DEMO's methodology which, although highly effective in calibrating the pseudo design candidates, might struggle in task environments with redundancy in design features.

Summary. The results presented in Tables 4 and 5 collectively validate DEMO's efficacy across both continuous and discrete optimization tasks, providing further support for answering $Q1$ affirmatively.

Table 5: Experimental results on discrete tasks, and ranking on all tasks for comparison.

Method	TF Bind 8	TF Bind 10	NAS	Rank Mean	Rank Median
$\mathcal{D}$(**best**)	0.439	0.467	0.436		
BO-qEI	0.439 ± 0.000	0.467 ± 0.000	0.544 ± 0.099	9.4/19	10/19
CMA-ES	0.537 ± 0.014	0.484 ± 0.014	$\mathbf{0.591 \pm 0.102}$	10.6/19	7/19
REINFORCE	0.462 ± 0.021	0.475 ± 0.008	-1.895 ± 0.000	13.7/19	18/19
Mean	0.539 ± 0.030	$\mathbf{0.539 \pm 0.010}$	0.494 ± 0.077	8.3/19	8/19
Min	0.569 ± 0.050	0.485 ± 0.021	$\mathbf{0.567 \pm 0.006}$	7.3/19	8/19
COMs	0.439 ± 0.000	0.467 ± 0.002	0.525 ± 0.003	11.1/19	11/19
ROMA	0.555 ± 0.020	0.512 ± 0.020	0.525 ± 0.003	8.6/19	7/19
NEMO	0.438 ± 0.001	0.454 ± 0.001	$\mathbf{0.564 \pm 0.016}$	10.4/19	11/19
BDI	0.439 ± 0.000	0.476 ± 0.000	0.517 ± 0.000	10.4/19	10/19
IOM	0.439 ± 0.000	0.477 ± 0.010	-0.050 ± 0.011	11.0/19	10/19
ICT	0.551 ± 0.013	$\mathbf{0.541 \pm 0.004}$	0.494 ± 0.013	5.6/19	**4/19**
Tri-mentoring	$\mathbf{0.609 \pm 0.021}$	0.527 ± 0.008	0.516 ± 0.028	6.1/19	**4/19**
PGS	0.375 ± 0.014	0.443 ± 0.005	0.508 ± 0.017	12.0/19	12/19
CbAS	0.428 ± 0.010	0.463 ± 0.007	0.292 ± 0.027	16.3/19	16/19
Auto CbAS	0.419 ± 0.007	0.461 ± 0.007	0.217 ± 0.005	16.9/19	17/19
MIN	0.421 ± 0.015	0.468 ± 0.006	0.433 ± 0.000	9.3/19	12/19
DDOM	0.401 ± 0.008	0.464 ± 0.006	0.306 ± 0.017	11.9/19	13/19
BONET	0.505 ± 0.055	0.496 ± 0.037	0.571 ± 0.095	4.6/19	5/19
DEMO$_{(\text{ours})}$	0.533 ± 0.010	0.480 ± 0.003	$\mathbf{0.564 \pm 0.005}$	**4.4/19**	**4/19**

With a mean rank of $4.4/19$ and a median rank of $4/19$ in terms of the median normalized scores, DEMO stands out among 19 competing methods. This comprehensive performance underscores DEMO's capacity to integrate and leverage information from the distribution of existing designs and pseudo design candidates.

A.3 Sensitivity to the Choice of m

In Eq. (9), selecting a time m close to M results in $\boldsymbol{x}_{perturb}$ resembling random Gaussian noise, which introduces greater flexibility into the new design generation process. On the other hand, if m is closer to 0, the resulting design retains more characteristics of the pseudo design candidates. Thus, m serves as a critical hyperparameter in our methodology. This section explores the robustness of DEMO to various choices of m. We perform experiments on one continuous task, SuperC, and one discrete task, TF8, with m ranging from 0 to 1000 in increments of 100. As illustrated in Figure 3, DEMO generally outperforms the Diffusion-only and Grad-only methods. Nevertheless, overly extreme values of m, whether too high or too low, can diminish performance. Selecting an excessively low m causes the model to adhere too closely to the pseudo design candidates, while choosing an overly high m biases the model towards the distribution of existing designs, neglecting the guidance of pseudo design candidates. Choosing m from a mid-range effectively balances the influences from both the prior distribution and the pseudo design candidates, leading us to set $m = 600$ for all tasks.

A.4 Reliability Study

In this subsection, we assess the ability of DEMO to reliably produce superior designs compared to selected surrogate based methods and generative model based methods. To measure reliability, we compute the proportion of new designs that exceed the best scores in the offline dataset $\mathcal{D}$(**best**). The results are depicted in Figure 4. DEMO consistently outperforms Diffusion-only across all tasks, achieving notable improvements, particularly in the SuperC and NAS tasks. This confirms DEMO's enhanced reliability over the state-of-the-art generative model-based baseline in both continuous and discrete settings. We then extends the reliability study to compare DEMO with a gradient-based approach. When compared to Grad-only, DEMO demonstrates greater consistency in 5 out of 7 tasks. However, Grad-only outperforms DEMO in Levy and TF10 tasks, which can be attributed to the gradient-based method's tendency to generate new designs within a narrower distribution. While Grad-only achieves a higher proportion of higher-scoring new designs in these two tasks, DEMO generates new designs within a wider distribution and thus produces candidates with higher maximum scores, as evidenced in Table 2.

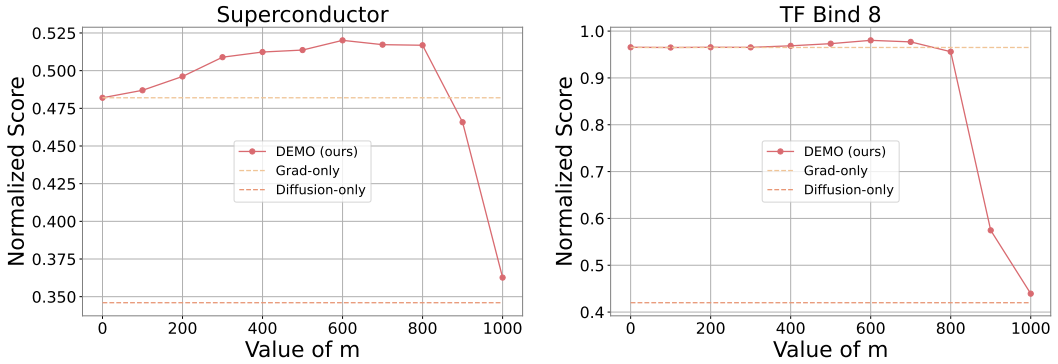

Figure 3: Selecting m near 0 results in generated designs that retains most properties of pseudo design candidates. Conversely, setting m near 1000 generates designs that align closely with the distribution of existing designs. Optimal designs are achieved by choosing m in the mid-range, effectively utilizing information from both the pseudo design candidates and the diffusion prior.

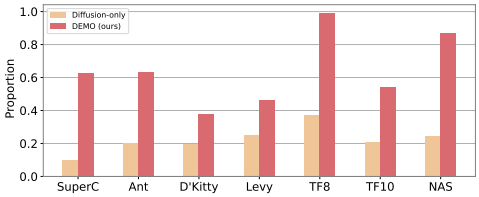

Figure 4: The proportion is calculated as the number of new designs which surpass $\mathcal{D}(\textbf{best})$ divided by the budget 128, indicating the reliability to consistently generate new higher-scoring designs. This figure demonstrates that DEMO is more reliable than Diffusion-only in all tasks.

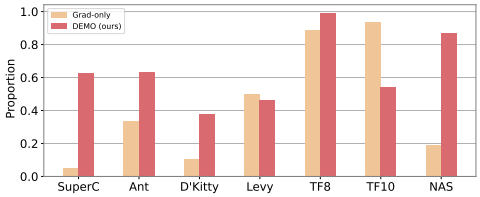

Figure 5: The proportion is calculated as the number of new designs which surpass $\mathcal{D}(\textbf{best})$ divided by the budget 128, indicating the reliability to consistently generate new higher-scoring designs. This figure demonstrates that DEMO is more reliable than Grad-only in $5/7$ tasks.

A.5 Related Works

In this subsection, we discuss the recent advancements in the offline model-based optimization problem, followed by diffusion-based editing techniques.

A.5.1 Offline Model-based Optimization

Recent offline model-based optimization (MBO) techniques broadly fall into two categories: *(i)* those that employ gradient-based optimizations and *(ii)* those that create new designs via generative models. Gradient-based methods often employ regularization techniques that enhance either the surrogate model Yu et al. (2021); Trabucco et al. (2021); Fu & Levine (2021); Qi et al. (2022a) or the design itself Chen et al. (2023c;b), thus improving the model's robustness and generalization capacity. Some approaches involve synthesizing new data with pseudo labels Yuan et al. (2023); Chen et al. (2023a), where they aim to identify useful information from these synthetic data to correct the surrogate model's inaccuracies. Other approaches like PGS Chemingui et al. (2024) employs policy-guided gradient search approach that explicitly learns the best policy for a given surrogate model. The second category encompasses methods that learn to replicate the conditional distribution of existing designs and their scores, including approaches such as MIN Kumar & Levine (2020), CbAS Brookes et al. (2019), Auto CbAS Fannjiang & Listgarten (2020), DDOM Krishnamoorthy et al. (2023a), and BONET Krishnamoorthy et al. (2023b). These methods are known for their ability to generate designs by sampling from learned distributions conditioned on higher target scores.

A.5.2 DIFFUSION-BASED EDITING

Diffusion models have shown remarkable success in various generation tasks across multiple modalities, especially for their ability to control the generation process based on given conditions. For instance, recent advancements have utilized diffusion models for zero-shot, test-time editing in the domains of text-based image and video generation. SDEdit Meng et al. (2022) employs an editing strategy to balance realism and faithfulness in image generation. To improve the reconstruction quality, methodologies such as DDIM Inversion Song et al. (2022), Null-text Inversion Mokady et al. (2023) and Negative-prompt Inversion Miyake et al. (2023) concentrate on deterministic mappings from source latents to initial noise, conditioned on source text. Building on these, CycleDiffusion Wu & De la Torre (2023) and Direct Inversion Ju et al. (2023) leverage source latents from each inversion step and further improve the faithfulness of the target image to the source image. Following the image editing technique, several video editing methods Qi et al. (2023); Ceylan et al. (2023); Yang et al. (2023); Geyer et al. (2023); Cong et al. (2023); Zhang et al. (2024) adopt image diffusion models and enforce temporal consistency across frames, offering practical and efficient solutions for video editing. Inspired by the success of these editing techniques in the field of computer vision, DEMO distinguishes itself in the context of offline MBO by first leveraging the surrogate model to craft pseudo design candidates and then refining them toward the in-distribution area.

A.6 LIMITATIONS

We have demonstrated the effectiveness of DEMO across a wide range of tasks. However, some evaluation methods may not fully capture real-world complexities. For example, in the superconductor task Hamidieh (2018), we follow traditional practice by using a random forest regression model as the oracle, as done in prior studies Trabucco et al. (2022). Unfortunately, this model might not entirely reflect the intricacies of real-world situations, which could lead to discrepancies between our oracle and actual ground-truth outcomes. Engaging with domain experts in the future could help enhance these evaluation approaches. Nevertheless, given DEMO's straightforward approach and the empirical evidence supporting its robustness and efficacy across various tasks detailed in the Design-Bench Trabucco et al. (2022) and BayesO Benchmarks Kim (2023), we remain confident in its ability to generalize effectively to different contexts.

A.7 NEGATIVE IMPACTS

This study seeks to advance the field of Machine Learning. However, it's important to recognize that advanced optimization techniques can be used for either beneficial or detrimental purposes, depending on their application. For example, while these methods can contribute positively to society through the development of drugs and materials, they also have the potential to be misused to create harmful substances or products. As researchers, we must stay aware and ensure that our contributions promote societal betterment, while also carefully assessing potential risks and ethical concerns.